Temperature Dependence of Photoluminescence Spectra of Nondoped and Electron-Doped SrTiO₃: Crossover from Auger Recombination to Single-Carrier Trapping

Yasuhiro Yamada,[1] Hideki Yasuda,[1] Takeshi Tayagaki,[1] and Yoshihiko Kanemitsu[1,2,*]

[1]*Institute for Chemical Research, Kyoto University, Uji, Kyoto 611-0011, Japan*
[2]*Photonics and Electronics Science and Engineering Center, Kyoto University, Kyoto 615-8510, Japan*
(Received 6 February 2009; published 18 June 2009)

We report unusual photoluminescence (PL) behaviors in highly photoexcited SrTiO₃ crystals at low temperatures. The PL spectrum and dynamics show abrupt changes below 150 K in both nondoped and electron-doped SrTiO₃ samples. We clarified that the PL dynamics in both nondoped and electron-doped SrTiO₃ is well described by the same simple model involving single-carrier trapping, radiative bimolecular recombination, and nonradiative Auger recombination. The unusual temperature dependence of PL dynamics is caused by the crossover from Auger recombination at high temperatures to single-carrier trapping at low temperatures. We discuss the temperature-dependent PL dynamics in conjunction with the high carrier mobility of SrTiO₃ at low temperatures.

Perovskite oxides have long been a subject of interest because of their unusual magnetic, electric, dielectric, and optical properties [1,2]. SrTiO₃ is one of the most important and potentially useful perovskites, both from the viewpoint of fundamental physics and its potential for device applications. SrTiO₃ is a wide-gap semiconductor with a band gap energy of 3.2 eV. On the basis of electron doping, the electric properties of SrTiO₃ vary significantly from insulating to semiconducting, metallic, and even superconducting [3–5]. Doped or photogenerated carriers in SrTiO₃ show high mobility at low temperatures [6], which results in large conductivity and enhancement of the dielectric constant [7,8]. Moreover, the recent discovery of two-dimensional electron gases (2DEGs) of the LaAlO₃/SrTiO₃ heterointerface prompts further interest in SrTiO₃ [9–13]. Despite the insulating properties of SrTiO₃ and LaAlO₃, a metallic 2DEG system is formed at the interface. Unique electric and magnetic properties of the LaAlO₃/SrTiO₃ heterointerface, such as magnetoresistance and superconductivity, are observed at low temperatures [12,13]. Despite extensive studies on the electronic structures and electric properties of SrTiO₃ bulk crystals and heterostructures [3–23], the carrier dynamics that determines these unique low-temperature multifunctional properties remains unclear.

Photoluminescence (PL) spectroscopy is one of the most powerful methods for studying carrier dynamics of semiconductors. Quantitative evaluation of carrier dynamics provides further understanding of the unique low-temperature properties of SrTiO₃ bulk crystals and heterostructures. Much effort has so far been devoted to the understanding of low-temperature PL properties, and it is reported that a broad green PL band appears around 2.5 eV [6,14–16]. Extrinsic defects and impurities affect the green PL spectra and dynamics of SrTiO₃ crystals [16–19], and the intrinsic carrier dynamics has not yet been clarified at

low temperatures. Under intense photoexcitation, however, defect and impurity PL usually saturate, and a blue PL band appears in nondoped SrTiO₃ at room temperature [20]. The intrinsic carrier recombination processes determine the room-temperature blue PL band. A similar blue PL band has been observed in electron-doped SrTiO₃ [21] and LaAlO₃/SrTiO₃ heterointerfaces [22]. Understanding of the blue PL dynamics provides a further insight into carrier recombination processes behind SrTiO₃ bulk crystals and SrTiO₃-based heterostructures.

In this Letter, we study the PL dynamics of highly excited SrTiO₃ over a wide range of temperature from 10 to 450 K and report the first observation of unusual PL behaviors at low temperatures. At around 150 K, the PL dynamics shows abrupt change in both nondoped and electron-doped SrTiO₃, and the PL spectrum changes in electron-doped SrTiO₃. The PL dynamics at all temperatures measured in both nondoped and electron-doped SrTiO₃ samples is well explained by the simple model involving single-carrier trapping, bimolecular radiative recombination, and nonradiative Auger recombination. We clarify that the crossover from Auger recombination at high temperatures to single carrier trapping at low temperatures plays a crucial role in temperature-dependent PL dynamics in SrTiO₃.

We used commercially available nondoped SrTiO₃ and electron-doped SrTi₁₋ₓNbₓO₃ ($x = 0.01$ and 0.02) single crystals (Furuuchi Chemical Co.). Nondoped samples were annealed under oxygen flow for 24 h at 700 K to reduce oxygen vacancies. All samples were 0.5 mm thick. Time-resolved PL spectra were measured with a time resolution of 40 ps using a streak camera and a monochromator. The excitation light source was an optical parametric amplifier system based on a regenerative amplified mode-locked Ti:sapphire laser with a pulse duration of 150 fs and a repetition rate of 1 kHz. The excitation photon energy was

3.54 eV. The laser spot size on the sample surface was measured carefully using the knife-edge method. Measurements were performed over a wide range of temperature from 10 to 450 K.

Figure 1(a) shows the time-gated (0–8 ns) and time-integrated PL spectra of nondoped $SrTiO_3$ at 10 and 300 K under an excitation density of 8.9 mJ/cm^2. The broad blue and green PL intensities are normalized by their peak intensities for comparison. At 300 K, a broad blue PL band appears at around 2.9 eV in the time-gated PL spectrum, and this time-gated PL spectrum shows good accordance with the time-integrated PL spectrum. The decay time of the broad blue PL band is 1–30 ns at 300 K, and it increases with a decrease of the laser intensity [20]. In contrast, three components are observed at 10 K: the time-gated PL spectrum shows a sharp peak at 3.2 eV and a broad band at around 2.9 eV, and the time-integrated PL spectrum shows a green broad PL band at 2.5 eV. The green PL shows a long decay time of milliseconds, and its initial states were assigned to impurity centers or self-trapped excitons [14–16].

The temperature dependence of the blue and green PL intensities is shown in Fig. 1(b). Here, we distinguished the broad blue PL spectra from the broad green PL spectra using the time-gated PL spectra, because the 0–8 ns integration interval of the time-gated PL spectra is much shorter than the millisecond decay time of the green PL and is comparable to or longer than the nanosecond decay time of the blue PL. The green PL intensity is obtained by subtracting the blue PL band from the time-integrated spectrum. With decreasing temperature below 150 K, the green PL intensity increases abruptly, while the blue PL intensity decreases. This behavior indicates that the near band-edge carriers for blue PL transform rapidly into the deep state for green PL and this transfer rate is temperature dependent.
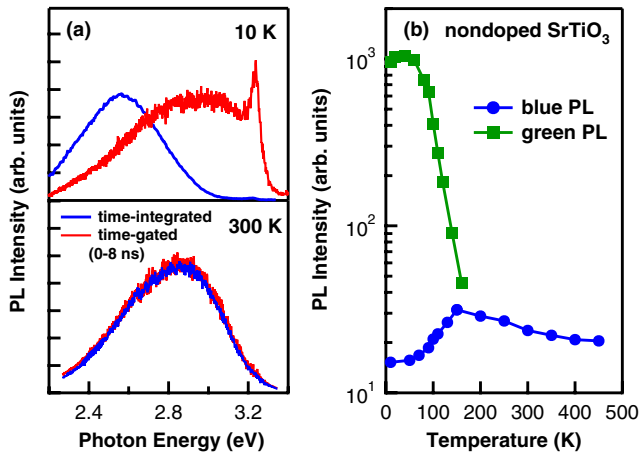
Figure 2 shows the decay curves of blue PL in nondoped $SrTiO_3$ at 10, 100, 200, and 400 K under an excitation density of 8.9 mJ/cm^2. The decay profiles have two decay components: a nonexponential fast decay with a subnanosecond time constant and a single-exponential slow decay with a time constant of several nanoseconds. These decay dynamics can be well explained by the rate equation of photocarriers. When the densities of photoexcited electrons and holes are equal (photocarrier density, n), the rate equation for the photocarriers can be simplified and written as follows [20,23,24]:

$$\frac{dn}{dt} = -An - Bn^2 - Cn^3, \qquad I_B \propto Bn^2, \qquad (1)$$

where A, B, and C represent the nonradiative single-carrier-trapping rate, radiative bimolecular recombination coefficient, and nonradiative Auger recombination coefficient, respectively. I_B denotes the blue PL intensity and is proportional to the square of the photocarrier density. The B coefficient is negligibly small because of the low PL efficiencies of the $SrTiO_3$ samples. The PL dynamics shows single-exponential decay in the low carrier density region and nonexponential decay due to Auger recombination in the high carrier density region. The solid curves in Fig. 2 are given by Eq. (1), and the experimental results are well described by the above simple rate equation. The fast and slow components in Fig. 2 are contributed by the Auger recombination (C coefficient) and single-carrier trapping (A coefficient), respectively. The inset shows an enlarged view of the PL decay profiles in the subnanosecond region at 10 and 400 K. At 10 K, the PL intensity decays slower than at 400 K, reflecting the reduction in the C coefficient with decreasing temperature.

The PL decay curves at all temperatures are well reproduced by the same rate equation, as shown in Fig. 2. The A and C coefficients are obtained as the best-fit parameters, and are summarized as a function of temperature in Fig. 3. The A coefficient shows an abrupt increase below 150 K,
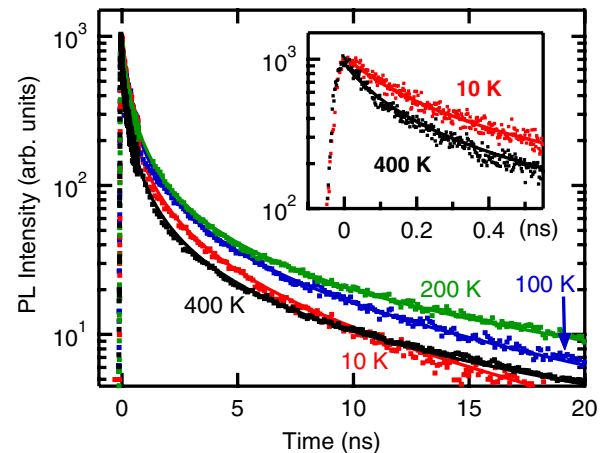

FIG. 1 (color online). (a) Time-gated (0–8 ns) and time-integrated PL spectra of nondoped $SrTiO_3$ at 10 and 300 K. (b) Temperature dependence of the PL intensities of the broad blue and green PL bands.

FIG. 2 (color online). PL decay curves of nondoped $SrTiO_3$ at 10, 100, 200, and 400 K. The inset shows an enlarged view of PL decay profiles in the subnanosecond region at 10 and 400 K.
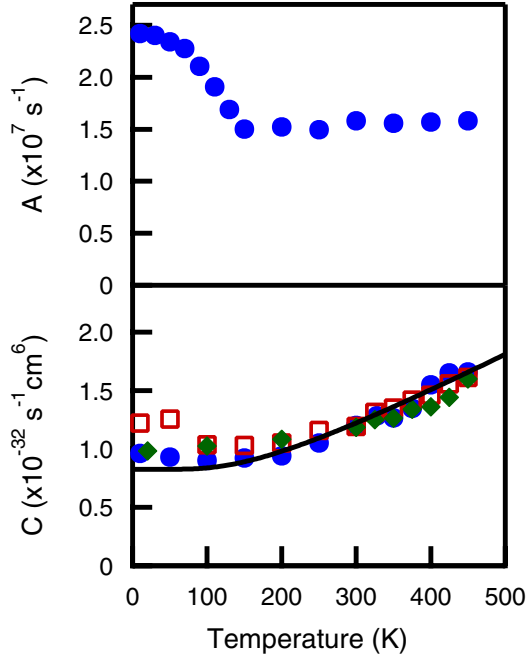
FIG. 3 (color online). Temperature dependence of the A and C coefficients obtained from the PL dynamics of nondoped SrTiO$_3$ (circles), SrTi$_{0.99}$Nb$_{0.01}$O$_3$ (squares), and SrTi$_{0.98}$Nb$_{0.02}$O$_3$ (diamonds). The solid curve shows the fitting result using Eq. (2).

corresponding to the increase in intensity of green PL and decrease in that of blue PL [see Fig. 1(b)]. This coincidence indicates that the abrupt increase in single-carrier trapping is due to rapid carrier relaxation into the deep state for the green PL band. In addition, the Hall measurement revealed that the electron mobility increases below 100 K [9,12,25]. Then, we conclude that the large mobility of the carriers enhances the carrier-trapping rate at low temperatures.

In contrast to the A coefficient, the C coefficient shows no significant change at 150 K. The C coefficient increases with increasing temperature at higher temperatures, while it remains almost constant at lower temperatures. This temperature dependence corresponds to the gradual decrease in intensity of blue PL with increasing temperature above 150 K. The temperature dependence of the Auger coefficient of semiconductors is usually described by a phonon-assisted Auger recombination model [26], in which the Auger coefficient is proportional to the sum of phonon emission and absorption rate:

$$C \propto 2N_{\text{phonon}} + 1 = \frac{\exp(\hbar\omega/kT) + 1}{\exp(\hbar\omega/kT) - 1}, \quad (2)$$

where $\hbar\omega$ is the energy of the phonon involving Auger recombination. This model is accepted in many bulk semiconductors (e.g., silicon [27]). We fitted the Auger coefficient obtained by PL dynamics of nondoped SrTiO$_3$ using Eq. (2). The solid curve in Fig. 3 shows the fitting results. The obtained best-fit parameter $\hbar\omega$ is 40 meV, which is very close to the energy of the zone boundary TO$_3$ phonon

of 41 meV [28]. Intrinsic Auger recombination determines the PL decay dynamics over a wide temperature range.

To gain a deeper understanding of the temperature-dependent PL dynamics of SrTiO$_3$, we examined the temperature dependence of the PL spectrum and decay in electron-doped SrTiO$_3$. Figure 4(a) shows the time-gated (0–8 ns) PL spectra of SrTi$_{0.99}$Nb$_{0.01}$O$_3$ at different temperatures. The excitation density of 0.12 mJ/cm^2 is so weak that the Auger recombination between photocarriers is negligibly small. The blue PL band is observed at 300 K. However, the blue PL band shows a sudden reduction and green PL appears below 150 K. At 10 K, the PL peak is located at 2.5 eV and the spectrum shape is almost identical to the green PL band in nondoped SrTiO$_3$. The PL dynamics in electron-doped SrTiO$_3$ at room temperature is dominated by the Auger recombination of doped carriers and photocarriers [20]. In this case, the PL decay curves are given by single-exponential decays and their decay rates are given by

$$\tau^{-1} = 2A + CN_e^2, \quad (3)$$

where N_e is the density of doped electrons. Figure 4(b) shows the PL decay profiles in SrTi$_{0.99}$Nb$_{0.01}$O$_3$ at 50, 250, and 450 K, where the PL intensity is integrated over the spectrum. All PL dynamics show single-exponential decay curves with a time constant of a few nanoseconds. The temperature dependence of the decay rate τ^{-1} is shown in the inset of Fig. 4(b). At high temperatures, the decay rate decreases monotonically with reducing temperature, and changes abruptly at 150 K. This temperature dependence suggests that at high temperatures the decay dynamics is determined by the Auger recombination, while at low temperatures below 150 K the single-carrier trapping dominates the decay dynamics.

While the green PL in nondoped SrTiO$_3$ shows nonexponential decay with a decay time of a few milliseconds at 10 K (data not shown), the green PL in electron-doped
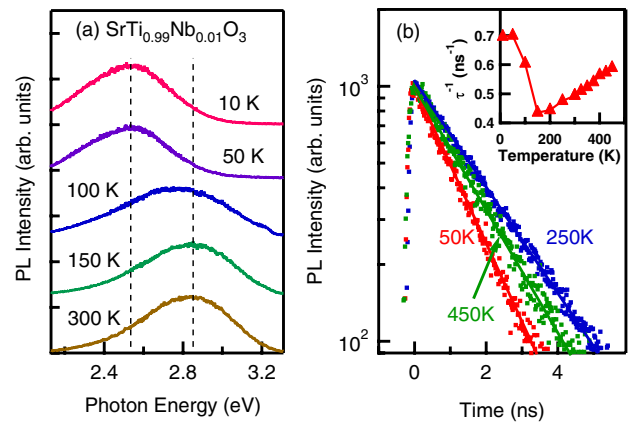

FIG. 4 (color online). (a) PL spectra of SrTi$_{0.99}$Nb$_{0.01}$O$_3$ at 10, 50, 100, 150, and 300 K. (b) PL decay curves of SrTi$_{0.99}$Nb$_{0.01}$O$_3$ at 50, 250, and 450 K. Inset: Temperature dependence of the decay rates τ^{-1}.

SrTiO$_3$ decays in a few nanoseconds [Fig. 4(b)]. These observations indicate that the fast green PL decay of electron-doped SrTiO$_3$ at low temperatures is determined by the decay rate described in Eq. (3). Although the PL spectral shape in electron-doped SrTiO$_3$ is different from that of nondoped SrTiO$_3$ at low temperatures, we attempt to determine the C coefficient from PL dynamics of electron-doped SrTiO$_3$ using Eq. (3). The C coefficient obtained by the PL dynamics of electron-doped SrTiO$_3$ is shown in Fig. 3, where we assumed that the carrier-trapping rate in electron-doped SrTiO$_3$ follows the same temperature dependence as nondoped SrTiO$_3$. These observations indicate that our model described by Eq. (1) works well in both electron-doped and nondoped SrTiO$_3$ over a wide temperature range.

As mentioned above, the green PL decay time of non-doped SrTiO$_3$ ($\tau \sim$ ms) is much larger than that of electron-doped SrTiO$_3$ at low temperatures. In nondoped SrTiO$_3$, the blue PL decreases slightly at low temperatures, while the blue PL in electron-doped SrTiO$_3$ disappears below 150 K. The blue PL intensity follows $I_B \propto BN_e p$, where p is photoexcited hole density [20]. Since the doped electron density N_e is almost independent of temperature [4], the PL dynamics of electron-doped SrTiO$_3$ is determined by the dynamics of photoexcited holes. We conclude that rapid energy relaxation of holes occurs into the deep states and the hole density abruptly decreases at low temperatures below 150 K in electron-doped samples.

In conclusion, we studied the temperature dependence of carrier dynamics in nondoped and electron-doped SrTiO$_3$ by means of time-resolved PL measurements. The simple model involving single-carrier trapping, bimolecular recombination, and Auger recombination well describes the PL dynamics at all temperatures in both nondoped and electron-doped SrTiO$_3$. The phonon-assisted Auger recombination determines the temperature-dependent PL dynamics. At low temperatures, rapid energy transfer occurs from the near band-edge state of blue PL to the deep state. The low-temperature PL dynamics is closely related to high mobility of carriers at low temperatures.

---

*Corresponding author.
kanemitu@scl.kyoto-u.ac.jp

[1] W. Eerenstein, N. D. Mathur, and J. F. Scott, Nature (London) **442,** 759 (2006).

[2] M. Imada, A. Fujimori, and Y. Tokura, Rev. Mod. Phys. **70,** 1039 (1998).

[3] H. P. R. Frederikse, W. R. Thurber, and W. R. Hosler, Phys. Rev. **134,** A442 (1964).

[4] O. N. Tufte and P. W. Chapman, Phys. Rev. **155,** 796 (1967).

[5] J. F. Schooley, W. R. Hosler, and M. L. Cohen, Phys. Rev. Lett. **12,** 474 (1964).

[6] T. Feng, Phys. Rev. B **25,** 627 (1982).

[7] M. Takesada, T. Yagi, M. Itoh, and S. Koshihara, J. Phys. Soc. Jpn. **72,** 37 (2003).

[8] T. Hasegawa, S. Mouri, Y. Yamada, and K. Tanaka, J. Phys. Soc. Jpn. **72,** 41 (2003).

[9] A. Ohtomo and H. Y. Hwang, Nature (London) **427,** 423 (2004).

[10] A. Tsukazaki, A. Ohtomo, T. Kita, Y. Ohno, H. Ohno, and M. Kawasaki, Science **315,** 1388 (2007).

[11] G. Herranz, M. Basletic, M. Bibes, C. Carrétéro, E. Tafra, E. Jacquet, K. Bouzehouane, C. Deranlot, A. Hamzić, J. M. Broto, A. Barthélémy, and A. Fert, Phys. Rev. Lett. **98,** 216803 (2007).

[12] N. Reyren, S. Thiel, A. D. Caviglia, L. Koukoutis, G. Hammerl, C. Richter, C. W. Schneider, T. Kopp, A. S. Rüetschi, D. Jaccard, M. Gabay, D. A. Muller, J. M. Triscone, and J. Mannhart, Science **317,** 1196 (2007).

[13] A. Brinkman, M. Huijben, M. Van Zalk, J. Huijben, U. Zietler, J. C. Maan, W. G. Van der Wiel, G. Rijnders, D. H. A. Blank, and H. Hilgenkamp, Nature Mater. **6,** 493 (2007).

[14] T. Hasegawa, M. Shirai, and K. Tanaka, J. Lumin. **87–89,** 1217 (2000).

[15] R. Leonelli and J. L. Brebner, Phys. Rev. B **33,** 8649 (1986).

[16] S. Mochizuki, F. Fujishiro, and S. Minami, J. Phys. Condens. Matter **17,** 923 (2005).

[17] S. Thiel, C. W. Schneider, L. F. Kourkoutis, D. A. Muller, N. Reyren, A. D. Caviglia, S. Gariglio, J.-M. Triscone, and J. Mannhart, Phys. Rev. Lett. **102,** 046809 (2009).

[18] K. Szot, W. Speier, R. Carius, U. Zastrow, and W. Beyer, Phys. Rev. Lett. **88,** 075508 (2002).

[19] A. Rubano, D. Paparo, F. Miletto, U. Scotti di Uccio, and L. Marrucci, Phys. Rev. B **76,** 125115 (2007).

[20] H. Yasuda and Y. Kanemitsu, Phys. Rev. B **77,** 193202 (2008).

[21] D. Kan, T. Terashima, R. Kanda, A. Masuno, K. Tanaka, S. Chu, H. Kan, A. Ishizumi, Y. Kanemitsu, Y. Shimakawa, and M. Takano, Nature Mater. **4,** 816 (2005).

[22] A. Kalabukhov, R. Gunnarsson, J. Börjesson, E. Olsson, T. Claeson, and D. Winkler, Phys. Rev. B **75,** 121404(R) (2007).

[23] H. Yasuda, Y. Yamada, T. Tayagaki, and Y. Kanemitsu, Phys. Rev. B **78,** 233202 (2008).

[24] P. T. Landsberg, *Recombination in Semiconductors* (Cambridge University Press, Cambridge, England, 1991).

[25] T. Ishikawa, M. Kurita, H. Shimoda, Y. Sakano, S. Koshihara, M. Itoh, and M. Takesada, J. Phys. Soc. Jpn. **73,** 1635 (2004).

[26] A. Haug, Solid State Commun. **28,** 291 (1978).

[27] K. G. Svantesson and N. G. Nilsson, J. Phys. C **12,** 5111 (1979).

[28] C. H. Perry, J. H. Fertel, and T. F. McNelly, J. Chem. Phys. **47,** 1619 (1967).